

## A Simple Analytical Model for the Interaction between the East Korean Warm Current and the Ulleung Warm Eddy

YOUNG HO SEUNG

*Department of Oceanography, Inha University, Incheon 402-751, Korea*

The offshore extension of the East Korean Warm Current (EKWC) mostly turns anti-cyclonically around the Ulleung Warm Eddy (UWE). This fact needs to be dynamically explained because a rectilinear stream past a circular cylinder is normally expected to have a flow pattern symmetric about the stream axis. For this purpose, a simple analytical model is presented in this paper. This model shows that the EKWC's tendency to be anti-cyclonic around the UWE is due to the anti-cyclonic circulation generated around the UWE. This tendency results from the geostrophic adjustment between the UWE and the ambient EKWC water. As the strength of the UWE decreases, relative to the EKWC, this model shows that the flow pattern gradually changes from circular to rectilinear.

**Key words:** East Korean Warm Current, Ulleung warm eddy, current-eddy interaction, analytical model

### INTRODUCTION

It has been known that a part of the Tsushima Warm Current forms the East Korean Warm Current (EKWC), once it enters the East Sea through the Korea Strait, and turns westward to flow along the Korean coast. The EKWC separates from the coast where it meets the southward flowing Cold Current. The separated EKWC flows, on average, eastward contributing to the formation of the polar front. The general circulation pattern of the East Sea is schematically shown in Fig. 1, which is supported by many observations (e.g., Lie *et al.*, 1995) and numerical experiments (e.g., Seung and Kim, 1993; Kim and Yoon, 1999). The horizontal temperature distribution at depth 100 m reflects well the general feature of the EKWC described above (Fig. 2).

An interesting point about the EKWC is its tendency to be anti-cyclonic around 37.4°N, 130.8°E after separating from the coast. In the schematic chart, this behavior is associated with the branching of the EKWC towards the NB (Fig. 1). In the historical temperature distribution at depth 100 m, the EKWC appears as a northward bending of the 5-9°C isotherms which otherwise run east-west off the Korean coast (Fig. 2). Though not shown here, this anti-

cyclonic behavior, called warm streamer, can be most clearly seen on the infrared satellite image in early spring (e.g., Shin *et al.*, 1995, Fig. 11). This is because the temperature contrast between the EKWC and the ambient waters is the greatest at this time of the year. The temperature distribution at depth 200 m where the EKWC is sufficiently weak shows that the anti-cyclonic behavior of the EKWC is associated with the presence of an isolated mass of warm water, i.e. the Ulleung Warm Eddy (UWE); the UWE generally penetrates downward more than 300 m. (Fig. 2). Since this water is centered, on average, near Ulleung Island (37.4°N, 130.8°E), it is often called the Ulleung Warm Eddy. However, the position of the UWE has been known to change from time to time around its average position (Kang and Kang, 1990). The UWE water has been believed to owe its high-temperature and high-salinity to the surrounding EKWC water which, after having been cooled in winter, is mixed downward (Kim, 1991). But most of the time, the waters of both the UWE and the EKWC have nearly the same density, constituting the upper layer against the underlying lower layer (Fig. 3).

This paper aims at demonstrating a part of the dynamical process arising from the interaction between the EKWC and the UWE with focus on the EKWC's tendency to be anti-cyclonic around the UWE. This work is significant in that there has not been any

---

\*Corresponding author: seung@inha.ac.kr

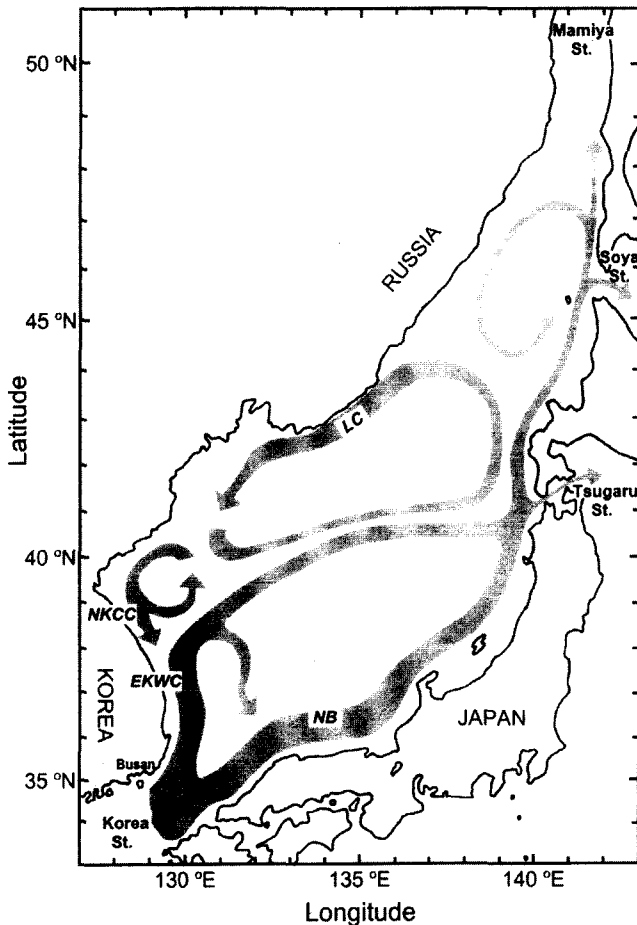


**Fig. 1.** Schematic diagram showing the surface circulation pattern of the Japan/East Sea with East Korean Warm Current (EKWC), Liman Current (LC), North Korean Cold Current (NKCC) and Nearshore Branch (NB). (after Senjyu, 1999)

dynamical explanation about this problem and that this tendency does not seem to be apparent since a rectilinear stream past a circular cylinder is normally expected to be symmetric about the stream axis. A simple analytical model is used in explaining this phenomenon. This paper is structured as follows: In section 2, the model is formulated and in section 3, the model results are analyzed and interpreted. Some discussion and conclusions are presented in section 4.

## MODEL FORMULATION

To demonstrate the EKWC's tendency to be anti-cyclonic around the UWE described in the previous section, a simple analytical model is constructed by idealizing the problem in the following way. Consider a two-layer ocean having an interface rising toward the north. In the upper layer, the current, flowing

eastward, is geostrophic. The lower layer is assumed to be infinitely deep and motionless. The problem concerns with the interaction between this mean flow field and a warm eddy, namely the UWE, embedded in it. However, the problem of how the warm eddy is generated is beyond the scope of the present study. Therefore, we take the following simple assumption about the existence of the eddy. Warm eddies have smaller potential vorticities than ambient water and are usually induced by an initial thickening of the water column. Thus, we assume that the eddy in its initial resting state has a layer thicker than that of the ambient upper layer by an initial amount. Later, the eddy and the ambient water will gravitationally adjust to each other while conserving the initial potential vorticities. Hence, an arbitrary initial state of the eddy is possible as long as the initially given potential vorticity is conserved. This type of approach is common in dynamical oceanography (e.g., Gill, 1982, p. 191–196).

The eddy is assumed to have a circular shape initially with radius  $a$  in the horizontal plane. Take the coordinate system with  $x$ - and  $y$ -axes pointing eastward and northward from the center of the eddy, and the  $z$ -axis upward from the surface (Fig. 4). Without the eddy, the upper layer has the thickness  $H_0$  at the origin with its lower interface sloping at  $-\alpha$ ; this is referred to as the basic state. In the basic state, the speed of the zonal geostrophic current,  $U$ , is  $U = \alpha g' / f_0$  where  $g'$  is the reduced gravity and  $f_0$  is the Coriolis parameter  $f$  at  $y=0$ . Here we take an approximation  $f = f_0 + \beta y \approx f_0$  because  $\beta L / f_0 \ll 1$ , where  $L$ , the meridional length scale considered in this problem, is only a few times of Rossby radius  $R_d$  that is defined by  $R_d = \sqrt{g' H_0} / f_0$ . (this approximation will become clear later.) Assume an initial form of the eddy which is thicker than the basic state layer thickness by an amount of  $\eta_0$ . We are interested only in the final state appearing after the gravitational adjustment of this initial state has ended. Let the deviation of the resulting (final state) upper layer thickness  $h$  from  $H_0$  be  $\eta$ , i.e.,  $h = H_0 + \eta$  (Fig. 4). To simplify the problem, we assume both  $\eta$  and  $\eta_0$  to be negligibly small compared with  $H_0$ , i.e.,  $\epsilon = O(\hat{\eta} / H_0) \ll 1$  where  $\hat{\eta}$  is the scale of either  $\eta$  or  $\eta_0$ . such that non-linear terms can be ignored. Note that the length scale of the disturbances is the Rossby radius  $R_d$  since the perturbations to the basic state arises from the geostrophic adjustment.

The governing equations of momentum and continuity for the inviscid and hydrostatic upper layer undergoing the adjustment are

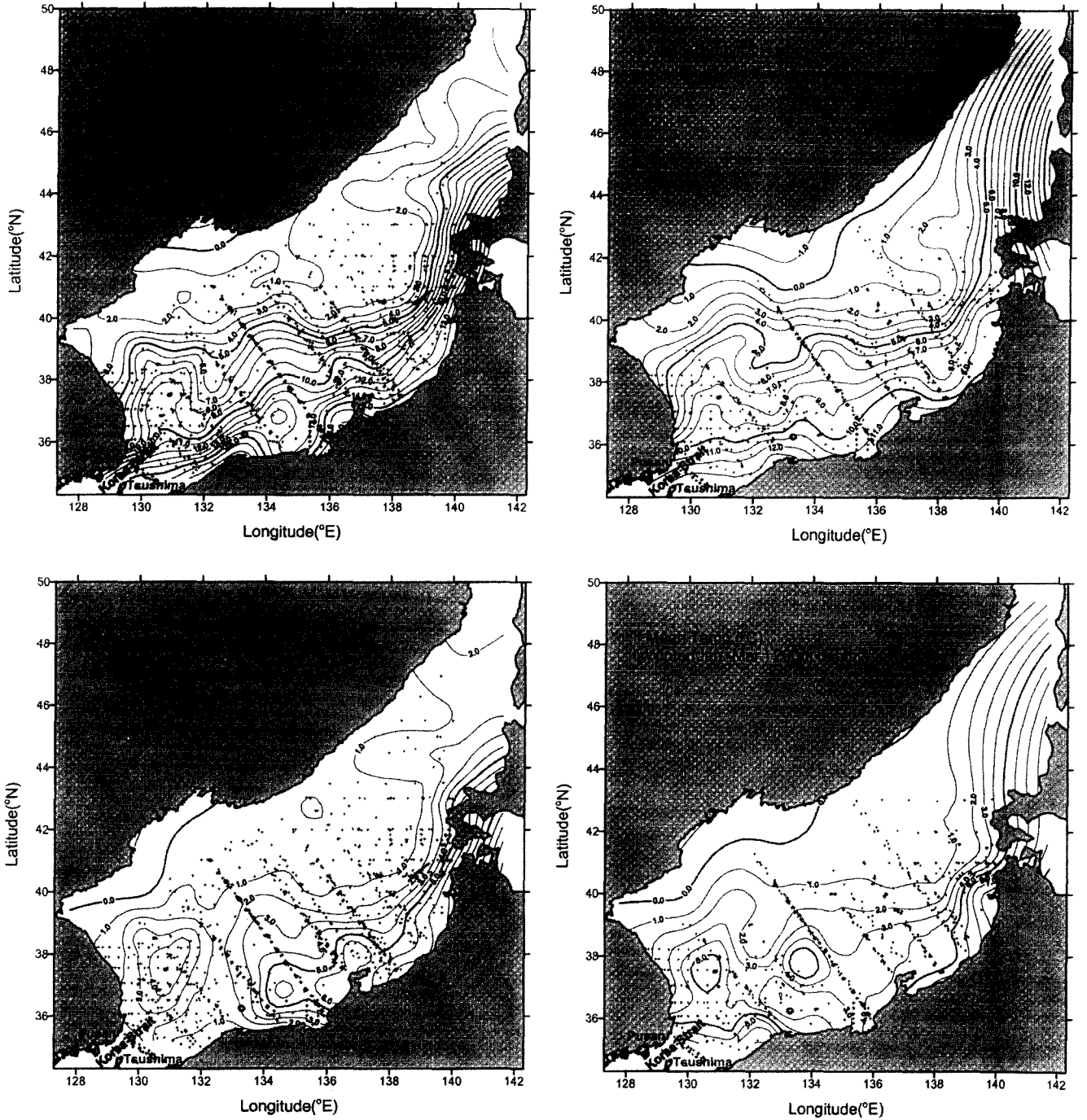


**Fig. 2.** Summer and winter mean temperatures at depths 100 m and 200 m constructed based on the historical data from Maizuru Marine Observatory, Japan and National Fisheries Research and Development Institute, Korea.

$$\frac{\partial u}{\partial t} - fv = -g' \frac{\partial \eta}{\partial x} \quad (1)$$

$$\frac{\partial v}{\partial t} + fu = -g' \frac{\partial \eta}{\partial y} \quad (2)$$

$$\frac{\partial \eta}{\partial t} + H_0 \left( \frac{\partial u}{\partial x} + \frac{\partial v}{\partial y} \right) = 0 \quad (3)$$

In (1) and (2), Coriolis force and pressure gradient are major terms. This means that  $(u, v)$  is of order  $g'\hat{\eta}/(f_0R_d)$ . Hence, the Rossby number (relative magnitude of non-linear term to Coriolis term) is of order  $\varepsilon = O(\hat{\eta}/H_0)$ . The  $\beta$ -effect is assumed still more negligible as considered above. Equations (1)-(3) are thus accurate to order  $\varepsilon$ . The problem of the adjust-

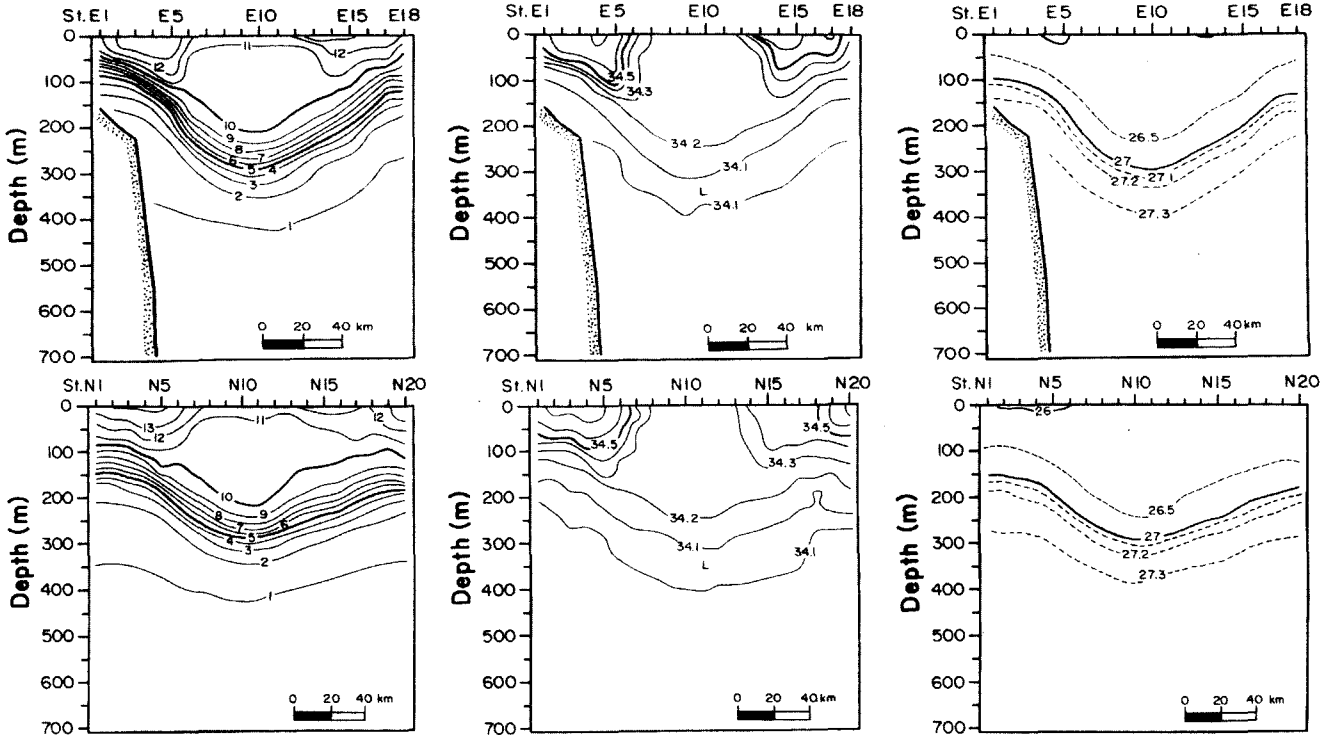


Fig. 3. Zonal and meridional sections of temperature ( $^{\circ}\text{C}$ ), salinity (psu) and density ( $\sigma_t$ ) (from left to right) crossing the UWE center obtained in April, 1993. Section E runs along latitude  $36.8^{\circ}\text{N}$  starting eastward from  $129.6^{\circ}\text{E}$  and section N runs along longitude  $130.6^{\circ}\text{E}$  starting southward from  $37.6^{\circ}\text{N}$ . (after KORDI, 1994)

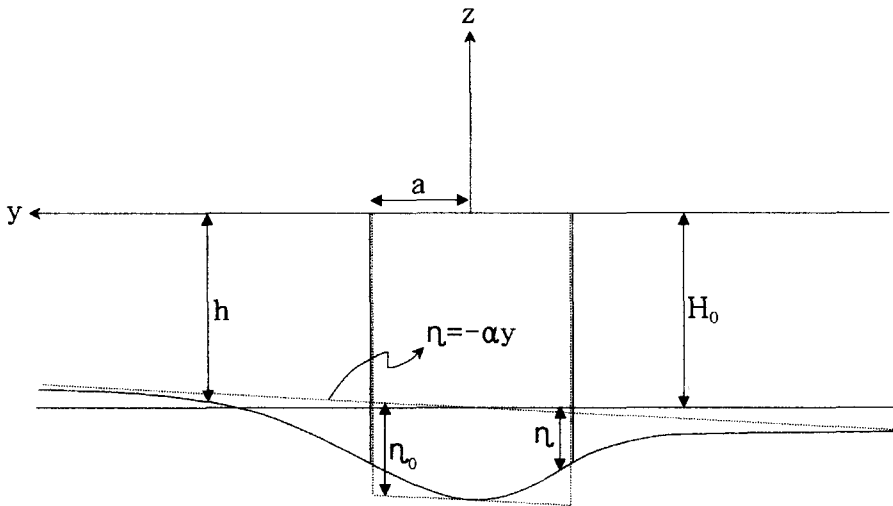


Fig. 4. Meridional section of the model ocean across the eddy center. Dotted and solid lines denote hypothetical initial state and final state, respectively. In the initial state, the interface is inclined in meridional direction with slope  $\alpha$  and the eddy is thicker than the ambient upper layer by  $\eta_0$ .

ment can then be analyzed in the same way as described by Gill (1982, p. 191-194). First, taking the curl of (1) and (2) using (3) leads to the linear form of the potential vorticity equation:

$$\frac{\partial}{\partial t} \left( \zeta - \frac{\eta}{H_0} \right) = 0 \quad (4)$$

where  $\zeta$  is the relative vorticity. Considering the initial state given above, this can be expressed in another form:

$$\zeta - \frac{\eta}{H_0} = \begin{cases} -\frac{\eta_0}{H_0} + \frac{\alpha y}{H_0} & r < a \\ \frac{\alpha y}{H_0} & r > a \end{cases} \quad (5)$$

where  $r$  is the radial distance from the origin. Next, taking the divergence of (1) and (2) using (3) results in an equation in terms of  $\eta$  and  $\zeta$ :

$$\frac{\partial^2 \eta}{\partial t^2} - g' H_0 \left( \frac{\partial^2 \eta}{\partial x^2} + \frac{\partial^2 \eta}{\partial y^2} \right) + f_0 H_0 \zeta = 0 \quad (6)$$

Eliminating  $\zeta$  from (5) and (6) leads to an equation in terms only of  $\eta$ :

$$\frac{\partial^2 \eta}{\partial x^2} + \frac{\partial^2 \eta}{\partial y^2} - \frac{\eta}{R_d^2} = \begin{cases} -\frac{\eta_0}{R_d^2} + \frac{\alpha y}{R_d^2} & r < a \\ \frac{\alpha y}{R_d^2} & r > a \end{cases} \quad (7)$$

Steady state solutions to (7) are obtained in each domain as follows:

$$\eta = \begin{cases} \eta_0 - \alpha y + c_1 I_0\left(\frac{r}{R_d}\right) + c_2 K_0\left(\frac{r}{R_d}\right) & r < a \\ -\alpha y + c_3 I_0\left(\frac{r}{R_d}\right) + c_4 K_0\left(\frac{r}{R_d}\right) & r > a \end{cases} \quad (8)$$

where  $I_0$  and  $K_0$  are the modified Bessel functions of zero order of the first and second kinds, respectively,  $c_1$  through  $c_4$  are constants of integration to be determined. For the solutions to have finite values,  $c_2$  and  $c_3$  must vanish. Applying the conditions that the solutions are continuous and have the same values at  $r=a$ , i.e.,  $\partial \eta(a^-)/\partial r = \partial \eta(a^+)/\partial r$  and  $\eta(a^-) = \eta(a^+)$  allows one to determine  $c_1$  and  $c_4$ . The final solution is

$$\eta = \begin{cases} \eta_0 - \alpha y - \frac{\eta_0 K_1(\xi) I_0(r/R_d)}{K_0(\xi) I_1(\xi) + K_1(\xi) I_0(\xi)} \\ -\alpha y + \frac{\eta_0 I_1(\xi) K_0(r/R_d)}{K_0(\xi) I_1(\xi) + K_1(\xi) I_0(\xi)} \end{cases} \quad (9)$$

where  $I_1$  and  $K_1$  are the modified Bessel functions of the first order and  $\xi = a/R_d$ . Note that the mass conservation of the eddy is correct to order  $\varepsilon$  irrespective of  $\eta$ , i.e.,

$$\int_0^{2\pi} \int_0^a (H_0 + \eta_0) r dr d\theta = \int_0^{2\pi} \int_0^a (H_0 + \eta) r dr d\theta + O(\varepsilon).$$

## MODEL RESULTS

Since the current in the steady state is geostrophic to order  $\varepsilon$ , the flow pattern can be represented by the distribution of  $\eta$ . For small disturbances, the transport between two points is proportional to the difference of  $\eta$  between them. As noted earlier, a circular transport is induced around the eddy, both on the inside and out. The amount of transport inside the eddy is measured by the difference of  $\eta$  between

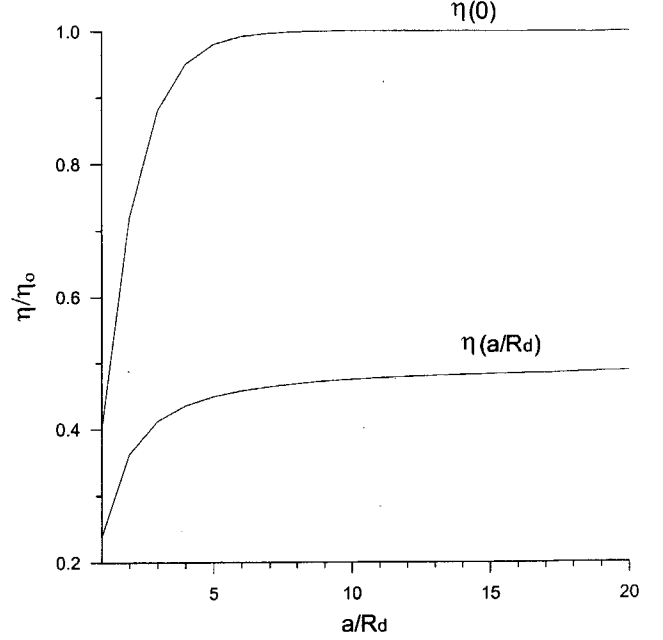


Fig. 5. Values of  $\eta$  at  $r=0$  and  $r=a$  as functions of the eddy size,  $a$ .

$r=0$  and  $r=a$  for  $\alpha=0$ , and outside the eddy by the difference between  $r=a$  and  $r=\infty$  (note that  $\eta=0$  at  $r=\infty$ ). These transports are proportional to the initial thickness of the eddy,  $\eta_0$ , as learned from (9). They also increase with the horizontal size of the eddy,  $a$ , although the rate of increase is significant only for small  $a$  (Fig. 5). When the basic state mean zonal flow is superimposed, the flow pattern becomes similar to that of the EKWC observed around the UWE (Fig. 2). This depends greatly on a non-dimensional number  $\alpha R_d/\eta_0$  which measures the importance of the mean zonal current relative to the circular transport induced by the eddy; as  $\alpha R_d/\eta_0$  increases, the flow becomes more rectilinear from circular (Fig. 6).

The flow can also be characterized by stagnation points. Their positions, denoted by  $(r_s, \theta_s)$  in the polar coordinate, are found by seeking the positions where  $\partial \eta/\partial r = 0$  and  $\partial \eta/\partial \theta = 0$  ( $\theta$  is the angle measured counter-clockwise). From (9), it can be learned that  $\theta_s = -\pi/2$  because  $y (=r \sin \theta)$  is the only term depending on  $\theta$ . Values of  $r_s$  obtained from (9) are shown as functions of  $\alpha R_d/\eta_0$  for three different  $a$ 's (Fig. 7). For each  $a$ , two stagnation points are formed, one inside and another outside the eddy. For the value  $\alpha R_d/\eta_0 = 0$ , both of them appear at the center of the eddy,  $r = 0$ , and at an infinitely large distance,  $r = \infty$ . As  $\alpha R_d/\eta_0$  increases, they approach toward  $r = a$ . For a given value of  $a$ , there is an upper limit of  $\alpha R_d/\eta_0$

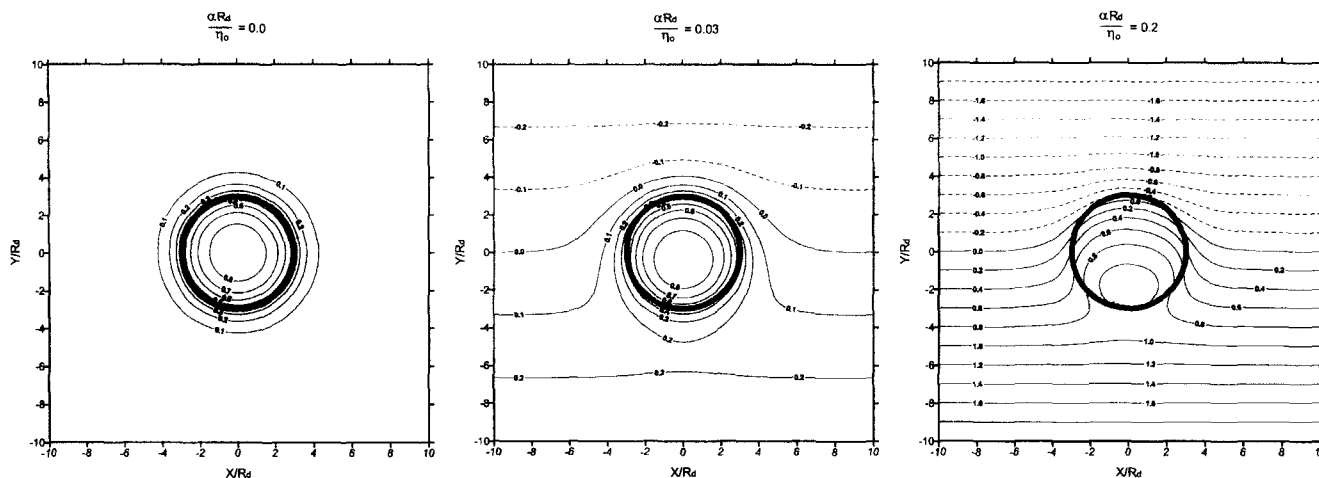


Fig. 6. Horizontal distribution of  $\eta$  for three different parameters  $\alpha R_d/\eta_0$ . Dotted lines denote negative values and thick lines drawn along  $r/R_d=3$  represent the initial boundary of the eddy.

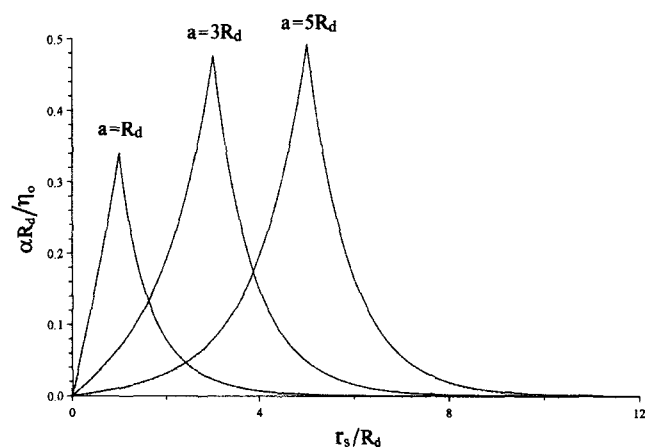


Fig. 7. Positions of the stagnation points,  $r_s$ , as functions of the parameter  $\alpha R_d/\eta_0$ , for eddies of three different sizes,  $a$ .

above which no stagnation point is formed. In this case, the flow is sufficiently rectilinear to prevent the formation of stagnation point. Overall, this model indicates that the observed anti-cyclonic behavior of the otherwise zonal EKWC is due to the circular transport induced by the presence of UWE, although the relative importance of the circular transport to the mean current cannot be quantified.

### DISCUSSION AND CONCLUSIONS

Using the simple analytic model, it is shown that the northward bending of the otherwise zonally-running isotherms near the Ulleung Island (Fig. 2) can be ascribed to the circular transport induced by the UWE. These isotherms are thought to represent the

streamlines of the offshore extension of the EKWC. The circular transport arising around the UWE results from the gravitational adjustment between the waters of the UWE and of the ambient EKWC. Hence, the EKWC's tendency to be anti-cyclonic around the UWE becomes more prominent with the strength of the UWE relative to that of the zonal EKWC.

It is noted that this model reveals only a part of the possible dynamical processes underlying the formation of the anti-cyclonic behavior of the EKWC as it assumes small interfacial disturbances. For a more accurate analysis, the non-linear effect should be included in future studies. Furthermore, the second order  $\beta$ -effect neglected in this model should be considered for more fundamental understanding of the interaction between the EKWC and the UWE as the UWE tends to move westward by this effect.

### ACKNOWLEDGEMENTS

This work was supported by INHA UNIVERSITY Research Grant (INHA-21977). Comments from Dr. Y. J. Ro and careful reading by Dr. J. C. Lee were helpful in revising the manuscript.

### REFERENCES

Gill, A.E., 1982. Atmosphere-Ocean Dynamics. Academic Press, 662 pp.  
 Kang, H.-E. and Y.Q. Kang, 1990. Spatio-temporal characteristics of the Ulleung Warm Lens. *Bull. Korean Fish. Soc.*, **23**: 407-415.  
 Kim, C.H. and J.H. Yoon, 1999. A numerical modeling of the upper and intermediate layer circulation in the East Sea. *J.*

- Oceanogr.*, **55**: 327–345.
- Kim, H.-R., 1991. The vertical structure and temporal variation of the intermediate homogeneous water near Ulleung Island. Master Thesis, Seoul National Univ., 84 pp. (in Korean).
- Korea Ocean Research and Development Institute, 1994. A study on the meso-scale warm eddy in the southwestern part of the East Sea. KORDI rep., BSPN 00222-721-1, 71 pp. (in Korean)
- Lie, H.-J., S.-K. Byun, I. Bang and C.-H. Cho, 1995. Physical structure of eddies in the southwestern East Sea. *J. Korean Soc. Oceanogr.*, **30**: 170-183.
- Senjyu, T., 1999. The Japan Sea Intermediate Water: Its characteristics and circulation. *J. Oceanogr.*, **55**: 111-122.
- Seung, Y.H. and K. Kim, 1993. A numerical modeling of the East Sea circulation. *J. Oceanol. Soc. Korea*, **28**: 292–304.
- Shin, H.-R., S.-K. Byun, C. Kim, S. Hwang and C.-W. Shin, 1995. The characteristics of structure of warm eddy observed to the northwest of Ulleungdo in 1992. *J. Korean Soc. Oceanogr.*, **30**: 39–56. (in Korean)
- 
- Manuscript received January 2, 2002  
Revision accepted February 6, 2002  
Editorial handling: Jae-Hak Lee